THE JOURNAL OF NAVIGATION (2019), **72**, 987–1006.
doi:10.1017/S0373463318001133

Improved Method for Single and Multiple GNSS Faults Exclusion based on Consensus Voting

Qieqie Zhang[1,2], Long Zhao[1,2] and Jianhua Zhou[1,2,3]

[1](*Science and Technology on Aircraft Control Laboratory, Beihang University, Beijing 100191, China*)
[2](*Digital Navigation Center, Beihang University, Beijing 100191, China*)
[3](*Beijing Satellites Navigation Center, Beijing 100094, China*)
(E-mail: buaa_dnc@buaa.edu.cn)

Receiver Autonomous Integrity Monitoring (RAIM) provides an integrity service for Global Navigation Satellite Systems (GNSS). The conventional RAIM algorithm is based on the assumption of a single fault and typically uses the forward-backward method, which is based on the *w*-test or correlation analysis methods, to exclude the faults. It is suitable for single fault detection and exclusion, while it can lead to inefficiency, can be misleading and can even fail in the exclusion of multiple faults. To solve this problem, an improved method based on consensus voting of the *w*-test and correlation analysis methods is presented. To verify the performance of the improved method, tests using Global Positioning System (GPS)/BeiDou System (BDS) data have been carried out in comparison with the conventional methods in terms of false and correct faults exclusion rate and computational complexity in the case of a different number of faults. Results show that the improved method has almost the same correct exclusion rate compared to the conventional RAIM in the case of a single fault. It is worth noting that the improved method has a higher correct exclusion probability and computational efficiency as well as a lower possibility of false exclusion in the case of multiple faults.

KEYWORDS

1. GNSS. 2. RAIM. 3. Fault detection and exclusion. 4. Multiple faults. 5. Consensus voting.

Submitted: 21 June 2018. Accepted: 22 December 2018. First published online: 27 February 2019.

1. INTRODUCTION. In Global Navigation Satellite Systems (GNSS), the satellite signals are extremely susceptible to the surrounding environment and human factors, such as multipath in urban canyons and spoofing. Therefore, it is rather difficult to guarantee accuracy and reliability of positioning in applications concerning safety of human life. Integrity is defined by the International Civil Aviation Organization's GNSS Standards and Recommended Practices (SARPS), which is used to describe the availability and reliability of a navigation system (Innac et al., 2016). An integrity service can provide timely warnings to users when the system or certain parts of it are unreliable for navigation (Yang and Xu, 2016).

Receiver Autonomous Integrity Monitoring (RAIM) is a common method for providing an integrity service, which includes Fault Detection and Exclusion (FDE). Lee (1986) first proposed that Global Positioning System (GPS) integrity could be provided in the user receiver by using redundant measurement information in a range and position comparison scheme for fault detection. Following this work, many RAIM schemes have been proposed and studied. In general, range comparison (Lee, 1986), least squares residuals (Parkinson and Penina, 1988), parity vector (Sturza, 1988) and maximum solution separation (Brown and McBurney, 1988) are known as the conventional methods. The latter three methods have the same principle in that they perform a self-consistency check among redundant measurements using a statistical hypothesis test based on least squares residuals (Brown, 1992). One of the conventional RAIM algorithms is the "Snapshot" algorithm which is based on the current measurements. It is widely used due to it not needing to consider the pre-state and post-state of the navigation system. As the conventional methods are based on the assumption of a single fault, they have a high accuracy of FDE in the case of a single fault but an unsatisfactory performance in cases of multiple faults. In order to improve the performance of RAIM in multiple FDE, some researchers have proposed to use *a priori* knowledge to achieve FDE. For example, McBurney and Brown (1989) and Ren and Ching-Fang (1995) proposed to use a Kalman filter to achieve GPS integrity monitoring. Yoo et al. (2012) proposed a new method to achieve GPS fault detection and isolation by comparing the measured pseudorange and the predicted pseudorange information obtained by a pseudorange prediction model. In addition, Yang et al. (2014) proposed to use supplementary information provided by external sensors to achieve integrity monitoring. These methods can improve the ability of FDE in the case of multiple faults. However, the performance of the prior knowledge-based FDE methods depends on the accuracy of prior error estimation and the speed of detection is slow, and for the methods based on supplementary sensor information, the reliability and accuracy of the sensor needs to be obtained in advance.

Using conventional RAIM algorithms as the basis, some improved solutions have been proposed. Hewitson and Wang (2006) presented an extended *w*-test method for the simultaneous removal of multiple outliers in measurements. Ni et al. (2007) and Knight et al. (2009) proposed an improved scheme assuming two satellite faults and Knight et al. (2010) further extended this reliability theory so that it can be applied to detect multiple faults. Cao et al. (2013) introduced an improved RAIM algorithm based on a parity vector method, which can effectively improve the availability of fault detection in the case of one or two faults. Yang et al. (2013) extended the theory of outlier separability to the general case, where there are multiple alternative hypotheses. Joerger and Pervan (2014) developed a new Chi-squared (Chi2) RAIM approach which can improve the performance of FDE in the case of two faults. Wang (2015) proposed an improved RAIM algorithm for two simultaneously faulty satellites on the basis of a QR-decomposition on a fault features plan. These methods can improve the performance of RAIM in the case of two faults to some degree, but in the case of more than two faults, there is no significant improvement in performance. In order to exclude multiple faults as accurately as possible, conventional RAIM algorithms typically use the forward-backward method based on the *w*-test to exclude the faults (Kuusniemi et al., 2007), but the method often misleads, fails to identify the fault and has a low computational efficiency. In view of the shortcomings of the *w*-test-based fault identification method, some researchers have proposed to use correlation analysis methods to detect and locate faults (Bei et al., 2010; Hu et al., 2014). However, in some cases, for

https://doi.org/10.1017/S0373463318001133 Published online by Cambridge University Press

example, when the correlation is not significant due to the interaction of multiple outliers, the correlation analysis method cannot get any better results (Tang et al., 2011). In order to improve the performance of RAIM in regard to single and multiple faults, we studied the traditional fault exclusion methods and proposed an improved method based on consensus voting of the *w*-test and correlation analysis methods.

We first introduce the error model of least squares estimation and describe the methods of fault detection. Then we present and discuss the conventional fault exclusion methods including the *w*-test and the correlation analysis methods and propose an improved method for single and multiple faults exclusion. Finally, we give test and experimental analysis and summarise the findings and conclusions.

2. SINGLE POINT POSITIONING AND ERROR MODEL.

The code pseudorange measurement between the satellite and the receiver can be written as follows (Kaplan and Hegarty, 2006):

$$\rho = R + c(dt_r - dt_s) + \Delta I + \Delta T + \varepsilon \tag{1}$$

where ρ is the measurement pseudorange, R is the geometric distance between the receiver and the satellite, c is the speed of light, dt_r and dt_s are the receiver and satellite clock offset, respectively, ΔT and ΔI are the tropospheric and ionospheric delay corrections, respectively and ε is the sum of unmodeled measurement errors. For simplicity, Equation (1) does not specify parameters such effects as antenna phase centre, hardware delays, multipath and windup angle.

According to Equation (1), the navigation equations system of Single Point Positioning (SPP) can be written in compact form as:

$$\boldsymbol{L} = \mathbf{A}\mathbf{x} + \boldsymbol{\varepsilon} \tag{2}$$

where $\boldsymbol{L}$ is an measurement vector containing the residuals between the measured and predicted pseudoranges. The elements of $\boldsymbol{L}$ can be obtained by:

$$L^i = \rho^i - R_0^i + cdt_s^i - \Delta I^i - \Delta T^i \tag{3}$$

The superscript i indicates the i-th satellite, L^i is the corresponding measurement, R_0 is the initial value of geometric distance and $\boldsymbol{A}$ is the design matrix containing the receiver-satellite geometry. $\boldsymbol{x}$ is the estimated parameters vector, for the single system, which is defined as follows:

$$\boldsymbol{x} = (dx, dy, dz, \delta t_r)^T \tag{4}$$

where (dx, dy, dz) indicates the deviation between the true and approximate coordinates and δt_r is the receiver clock offset. For multiple systems, such as a GPS/BeiDou System (BDS) combined system, there is an Inter-System Bias (ISB) between GPS and BDS due to the different coordinate frames and time references. In general, the difference of the coordinate frame between GPS and BDS has little influence on SPP and could be ignored. Thus, the ISB shows up as the receiver clock difference between GPS and BDS, which is usually treated as a parameter to be estimated (Chen et al., 2016; Pan et al., 2017).

It is assumed that the measurement error is a normally distributed random variable with zero mean and a standard deviation of σ_i. For the i-th visible satellite, the measurement

https://doi.org/10.1017/S0373463318001133 Published online by Cambridge University Press

variance σ_i^2 of L^i can be obtained by (Takasu and Yasuda, 2013):

$$\sigma_i^2 = R_r(a_\sigma^2 + b_\sigma^2 / \sin El_r^s) + \sigma_{eph}^2 + \sigma_{ion}^2 + \sigma_{trop}^2 + \sigma_{bias}^2 \tag{5}$$

where R_r is the code/carrier-phase error ratio, a_σ and b_σ are the carrier-phase error factors (m), El is the elevation angle of the satellite, σ_{eph} is the standard deviation of ephemeris and clock errors (m), σ_{ion} is the standard deviation of the ionosphere correction model error (m), σ_{trop} is the standard deviation of the troposphere correction model error (m) and σ_{bias} is the standard deviation of the code bias error (m). According to the principle of weighted least squares, the estimated parameters vector $\hat{\boldsymbol{x}}$ can be calculated as follows:

$$\hat{\boldsymbol{x}} = \left(\boldsymbol{A}^T\overline{\boldsymbol{P}}\boldsymbol{A}\right)^{-1}\boldsymbol{A}^T\overline{\boldsymbol{P}}\boldsymbol{L} \tag{6}$$

where:

$$\overline{\boldsymbol{P}} = diag\left\{1/\sigma_1^2, 1/\sigma_2^2, \ldots, 1/\sigma_m^2\right\} \tag{7}$$

which is the diagonal weight matrix, and each element is the reciprocal of the variance of each measurement.

The residual vector $\boldsymbol{v}$ is defined as the difference between measurements $\boldsymbol{L}$ and the fitted model $\boldsymbol{A}\hat{\boldsymbol{x}}$:

$$\boldsymbol{v} = \boldsymbol{L} - \boldsymbol{A}\hat{\boldsymbol{x}} \tag{8}$$

Substituting Equations (2) and (6) into Equation (8), the residual vector $\boldsymbol{v}$ can be written as:

$$\boldsymbol{v} = \boldsymbol{L} - \boldsymbol{A}\left(\boldsymbol{A}^T\overline{\boldsymbol{P}}\boldsymbol{A}\right)^{-1}\boldsymbol{A}^T\overline{\boldsymbol{P}}\boldsymbol{L} = (\boldsymbol{I} - \boldsymbol{Q})\,\boldsymbol{L} = \boldsymbol{S}\boldsymbol{\varepsilon} \tag{9}$$

where $\boldsymbol{Q}$ is an idempotent matrix, $\boldsymbol{I}$ is the identity matrix and $\boldsymbol{S} = \boldsymbol{I}\text{-}\boldsymbol{Q}$ is called the mapping matrix.

As can be seen from Equation (9), the residual vector $\boldsymbol{v}$ is the mapping of random error vector $\boldsymbol{\varepsilon}$ though the mapping matrix $\boldsymbol{S}$. There is a linear relationship between the measurement residual and the measurement error, so they should have the same random distribution characters. If there is an outlier in the measurement, it will be shown in the residual vector $\boldsymbol{v}$ through the mapping $\boldsymbol{S}$. Therefore, an outlier can be detected and identified by analysing the residual vector.

3. FAULT DETECTION METHOD. Fault detection is one of the important functions of RAIM, which is based on hypothesis testing. The hypothesis test is:

$$\begin{cases} H_0: & r \le T \\ H_1: & r > T \end{cases} \tag{10}$$

where r is the test statistic, T is the threshold, H_0 is the hypothesis that there is no fault and H_1 is the hypothesis that there are one or more faults. The process of fault detection is implemented by comparing the test statistic r and threshold T. If $r > T$, it indicates hypothesis H_1 is accepted, and a fault is detected.

https://doi.org/10.1017/S0373463318001133 Published online by Cambridge University Press

The Weighted Sum Squared of Residual (WSSR) calculated by Equation (9) is subject to a Chi-square distribution in the fault-free case, and non-central Chi-squared distribution in the faulty case (Parkinson and Penina, 1988). Hence the test statistic can be formulated as:

$$r = \frac{\boldsymbol{v}^T \overline{\boldsymbol{P}} \boldsymbol{v}}{\sigma_0^2} \sim \chi^2_{1-a,f} \quad (f = n - m) \tag{11}$$

where σ_0^2 is the prior variance factor, a is the significance level of the Chi-square test and f is the number of redundancies and is equal to the difference between the number of observations n and the number of estimated parameters m. It is determined whether there are faults by comparing the test statistic r and detection threshold T calculated by the significance level a.

Despite the use of the rigorous Chi-square testing procedures, there are still two types of error that can occur (Feng et al., 2006). A type I error occurs when the null hypothesis H_0 is true but is rejected. A type II error occurs when the null hypothesis H_0 is false but erroneously fails to be rejected. In fault detection, type I and II errors are also called false alert and missed detection, respectively. Their probabilities are expressed by the following equations (Sturza, 1988; Salos et al., 2014):

$$P_{FA} = P\left\{\mathrm{r} > T \mid H_0 : \mathrm{r} \sim \chi^2_f\right\} = 1 - CDF_{\chi^2_f}(T) \tag{12}$$

$$P_{MD} = P\left\{r \leq T \mid H_1 : r \sim \chi^2_{f,\lambda}\right\} = CDF_{\chi^2_{f,\lambda}}(T) \tag{13}$$

where CDF is the Cumulative Density Function; χ^2_f is the Chi-square distribution with degree of freedom f and $\chi^2_{f,\lambda}$ is the non-central Chi-squared distribution with non-central parameter λ.

As can be seen from Equations (12) and (13), P_{FA} is related to the threshold T, and the non-central parameter λ is related to P_{MD} and T. The relationships between them are shown in Figure 1. We can see that P_{FA} and P_{MD} are contradictory in the case that the non-central parameter λ is known. For example, P_{FA} decreases and P_{MD} increases with the increases of threshold T and vice versa. Moreover, if P_{FA} is known, then T can be determined. P_{MD} is only related to λ and decreases with the increases of λ and vice versa. Similarly, if P_{FA} and P_{MD} are known, the non-central parameter can be calculated by the following function (Knight et al., 2010):

$$\lambda_{\mathrm{det}} = \lambda(P_{FA}, P_{MD}, f) \tag{14}$$

where λ_{det} is called the minimum detectable non-centrality. According to the parameter λ_{det}, if there is a single fault in measurement, the Minimum Detectable Bias (MDB) of each pseudorange measurement can be determined by (Knight et al., 2009):

$$\nabla b_i = \frac{\lambda_{\mathrm{det}} \sigma_0}{\sqrt{P_{ii} S_{ii}}} \quad (i = 1, 2, \cdots, n) \tag{15}$$

where ∇b_i is the minimum detectable bias of the i-th pseudorange measurement; P_{ii} and S_{ii} are the elements in the i-th row and i-th column of $\boldsymbol{P}$ and $\boldsymbol{S}$, respectively. In regard to multiple faults, the MDB in the i-th pseudorange measurement is greater than or equal to the corresponding MDB for a single fault (Knight et al., 2010).

https://doi.org/10.1017/S0373463318001133 Published online by Cambridge University Press

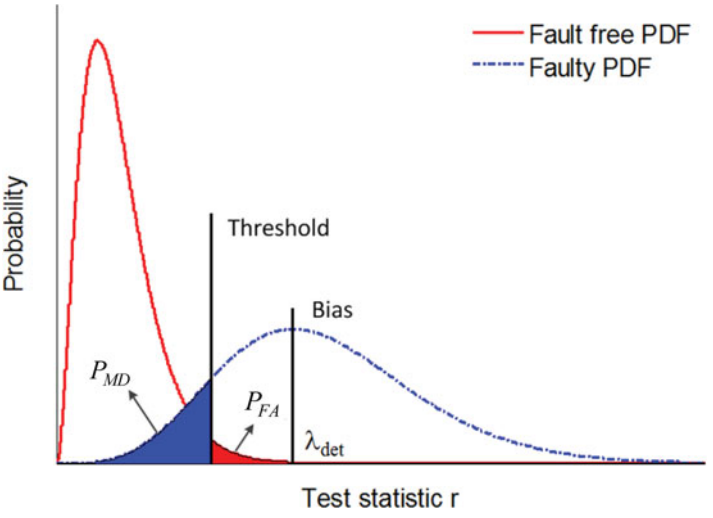

Figure 1. Relationship between the probability of false alert and missed detection.

The Chi-square test based on the weighted sum of the squared residuals is a commonly used method for detecting outliers. The performance of the Chi-square test depends on P_{FA} and P_{MD}. The probability of successful detection is determined by P_{FA}, and the sensitivity of fault detection is determined by P_{MD}.

4. FAULT EXCLUSION METHODS. When faults are detected by the Chi-square test, it is necessary to identify and exclude the faults to ensure the reliability and accuracy of positioning. Common RAIM algorithms typically use the forward-backward method based on the *w*-test or correlation analysis methods to identify and exclude the faults (Hewiston et al., 2004; Hewitson and Wang, 2006; Tang et al., 2011). First, the forward fault exclusion is performed, the possible faults are excluded one by one based on the identification results of the *w*-test or correlation analysis methods until no fault is detected, and then a backward check is made to ensure the excluded faults are correct.

4.1. *w-test method.* The *w-test* is a test of normality in frequentist statistics. It can be used to identify outliers in measurements under the assumption that measurement errors are normally distributed. The test statistic is defined as follows (Baarda, 1968; Hewiston et al., 2004; Hewitson and Wang, 2006):

$$\omega(i) = |v_i| / \sigma_{v_i} = |v_i| / \sigma_0 \sqrt{S_{ii}} \quad (i = 1, 2, \ldots, n) \tag{16}$$

where v_i is the i-th element of $\boldsymbol{v}$, $\sigma_{v_i} = \sigma_0 \sqrt{S_{ii}}$ is the standard deviation of v_i and $\omega(i)$ is the test statistic for the i-th measurement, which has a standard normal distribution in the fault-free case and has a non-central normal distribution in the presence of a fault. The critical value for $\omega(i)$ to be tested against is $N_{1-a/2}(0, 1)$. If $|\omega(i)| > N_{1-a/2}(0, 1)$, the i-th measurement is assumed to be an outlier. The test is carried out with respect to each measurement; if the maximum value of $\omega(i)(i = 1, 2, \cdots, n)$ exceeds the critical value, the corresponding measurement is deemed an outlier and is removed from the observation model.

https://doi.org/10.1017/S0373463318001133 Published online by Cambridge University Press

4.2. *Correlation analysis methods.* The correlation analysis methods are based on the degree of correlation between the measurement error ε and the residual vector $\boldsymbol{v}$ to identify the outlier. According to Equation (9), the relationship between $\boldsymbol{v}$ and $\boldsymbol{\varepsilon}$ can be expressed as follows (Tang et al., 2011):

$$\boldsymbol{v} = \boldsymbol{S}\boldsymbol{\varepsilon} = \begin{bmatrix} S_{11} & S_{12} & \cdots & S_{1n} \\ S_{21} & S_{22} & \cdots & S_{2n} \\ \vdots & \vdots & \ddots & \vdots \\ S_{n1} & S_{n2} & \cdots & S_{nn} \end{bmatrix} \boldsymbol{\varepsilon} = \boldsymbol{S}_1\varepsilon_1 + \boldsymbol{S}_2\varepsilon_2 + \cdots + \boldsymbol{S}_n\varepsilon_n \tag{17}$$

where $\boldsymbol{S}_i = \begin{bmatrix} S_{1i} & S_{2i} & \cdots & S_{ni} \end{bmatrix}^T \quad (i = 1, 2, \cdots, n)$ is the impact vector of the error $\boldsymbol{\varepsilon}_i$ on $\boldsymbol{v}$. This reflects the contribution of measurement errors $\boldsymbol{\varepsilon}_i$ to the residuals vector $\boldsymbol{v}$, that is, if L^i contains a gross error $\boldsymbol{\varepsilon}_i$ this will be mapped to $\boldsymbol{v}$ through $\boldsymbol{S}_i$. In this case, $\boldsymbol{v}$ is mainly affected by $\boldsymbol{S}_i$. Consequently, the correlation between $\boldsymbol{\varepsilon}$ and $\boldsymbol{v}$ can be replaced by the correlation between $\boldsymbol{S}_i$ and $\boldsymbol{v}$. There are two indicators used to characterise the degree of correlation: correlation coefficient and correlation distance. The calculation formulae for these indicators are (Bei et al., 2010; Filliben, 1975; Hu et al., 2014; Tang et al., 2011):

$$c(i) = \frac{\sum_{j=1}^{n} \left(S_{ji} - \overline{\boldsymbol{S}}_i\right)\left(v_j - \boldsymbol{v}\right)}{\sqrt{\left(\sum_{j=1}^{n} \left(S_{ji} - \overline{\boldsymbol{S}}_i\right)^2 \sum_{j=1}^{n} \left(v_j - \overline{\boldsymbol{v}}\right)^2\right)}} \quad (i = 1, 2, \cdots n) \tag{18}$$

$$d(i) = \sqrt{\frac{1}{n}\sum_{j=1}^{n} \left(S_{ij} - v_j\right)^2} \quad (i = 1, 2, \cdots n) \tag{19}$$

where $c(i)$ and $d(i)$ are the correlation coefficient and correlation distance, respectively. $\overline{\boldsymbol{S}}_i$ and $\overline{\boldsymbol{v}}$ are the mean values of $\boldsymbol{S}_i$ and $\boldsymbol{v}$ respectively. $\boldsymbol{S}_{ji}$ is the j-th element of the $\boldsymbol{S}_i$, and $\boldsymbol{v}_j$ is the j-th element of the $\boldsymbol{v}$. According to the principle of correlation analysis, we take the measurement corresponding to the maximum of the absolute value of correlation coefficient $c(i)$ or the minimum of correlation distance $d(i)$ as an outlier.

The forward-backward fault exclusion methods based on w-test (FDE-w), correlation coefficient (FDE-c) or correlation distance (FDE-d) all show a good performance under the situation of a single fault. However, in the case of multiple faults, the three methods often falsely identify or fail to exclude faults due to the combined effect of multiple faults, and the efficiency is lower. These problems will be illustrated in Section 6.

5. AN IMPROVED METHOD FOR FAULT EXCLUSIONS. As is known, the w-test, the correlation coefficient, and the correlation distance are three methods that can be used to identify faults. In the case of a single fault, the three methods all have a comparatively high correction identification ratio and should have the same identification result. In the case of multiple faults, since the three methods use different test statistics and judgment mechanisms, they might get different identification results. As shown in Table 1, there are three situations that may occur if fault identification is based on the three methods at

https://doi.org/10.1017/S0373463318001133 Published online by Cambridge University Press

Table 1. Three situations that may occur at each time fault exclusion based on the identification results of *w*-test and correlation analysis methods.

Situations	Conditions of satisfaction
I	$k1 = k2$ & $k2 = k3$
II	$k1 = k2$ || $k1 = k3$ || $k2 = k3$
III	$k1! = k2$ & $k1! = k3$ & $k2! = k3$

each time. In Table 1, $k1$, $k2$ and $k3$ indicate the identification results of *w*-test, correlation coefficient and correlation distance methods respectively.

On the basis of a consensus voting strategy (McAllister et al., 1990; Zhao et al., 2015), the *w*-test, the correlation coefficient, and the correlation distance methods can be used to identify the fault at each time fault exclusion. If the identification results of the three methods meet situation I, then they have a good consistency. In this case, since the correct identification probability of the three methods are higher than the probability of false identification, the probability that the three methods have the same wrong identification result will be very low. So, when the identification results of the three methods meet situation I, the probability that the identification result is a fault will be very high. If the identification results of the three methods meet situation II, only two of the three identification results are consistent. In this case, the probability that two methods have the same wrong identification result will be high. According to the significance test of the correlation coefficient, if the maximum correlation coefficient is significant at a given significance level, then the probability that the corresponding measurement is an outlier is high (Tang et al., 2011). In order to reduce the probability of a false identification in situation II, the significance of the correlation coefficient can be used as an additional condition. If the *w*-test and correlation coefficient, or the correlation distance and correlation coefficient methods have the same identification result, and the maximum correlation coefficient is significant, the probability that the identification result is a fault will also be high.

According to the above analysis, we propose an improved fault identification method based on consensus voting of the three methods under situations I and II, and the consensus voting model is given as follows:

$$Result = 1 \Rightarrow \begin{cases} k1 = k2 & || & k2 = k3 & c(i)_{\max} \geq c_d \\ k1 = k2 & \& & k2 = k3 & c(i)_{\max} < c_d \end{cases} \tag{20}$$

where $c(i)_{\max}$ denotes the maximum of $c(i)$ and c_d is the threshold value with significance level β, which can be calculated by the probability density function of the correlation coefficient (Filliben, 1975; DeGroot and Schervish, 2011):

$$f(c) = \frac{\Gamma\left(\frac{n-1}{2}\right)}{\sqrt{\pi}\Gamma\left(\frac{n}{2}-1\right)}\left(1-c^2\right)^{\frac{n-4}{2}} \tag{21}$$

where Γ is the gamma function. The threshold c_d can also be obtained by checking the correlation coefficient table with significance level β and degree of freedom $n-2$.

https://doi.org/10.1017/S0373463318001133 Published online by Cambridge University Press

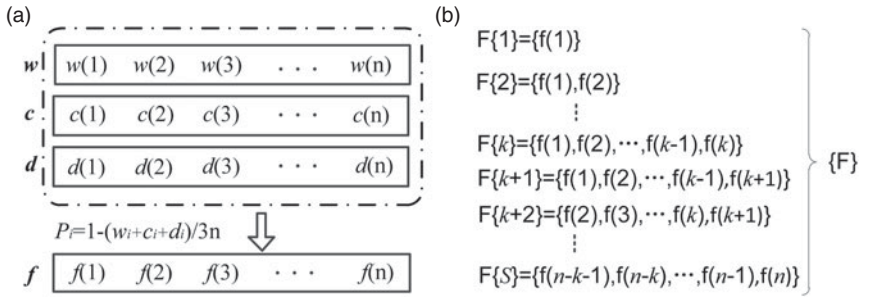

Figure 2. Schematic diagram of fault set construct.

When the identification results of the three methods meet situation III or meet situation II but do not satisfy Equation (20), we cannot determine which identification result of the three methods is indeed a fault. In this case, we exclude the faults by building the fault set {F} and traversing all subsets F{l}($l = 1, 2, \ldots, S$). In order to cover all possible combinations of faults and reduce the computation burden as much as possible, the fault set {F} is constructed based on the following principles: as shown in Figure 2(a), a vector $\boldsymbol{f}$ is obtained by first sorting all the observations according to the fault probability that is calculated by:

$$P_i = 1 - (w_i + c_i + d_i)/3n \tag{22}$$

where the subscript i indicates the i-th observation, w_i, c_i and d_i are the index values of the statistics corresponding to the i-th observation in vectors $\boldsymbol{w}$, $\boldsymbol{c}$, and $\boldsymbol{d}$, respectively. The fault set {F} can then be constructed according to $\boldsymbol{f}$, as shown in Figure 2(b). The size of {F} is $S = k - 1 + C(n, k)$, where $k = n - n_{\min}$ and $n_{\min}$ is the minimum number of observations required for FDE (for a single satellite system, $n_{\min} = 5$ and for a combined GPS/BDS system, $n_{\min} = 6$).

The flow chart of the improved faults detection and exclusion algorithm (FDE-u) is shown in Figure 3. The steps of the algorithm can be described as follows:

Step 1: Determine whether the FDE function is available according to the number of satellites or observations. If $n<n_{\min}$, fault detection and exclusion are unavailable or failed.

Step 2: Fault detection according to Chi-square test. Update the test parameters r according to Equation (11) and detection threshold T according to the Chi-square test table. If $r >$ T, it indicates that some faults are detected. Otherwise, there are no faults detected or faults exclusion succeeded.

Step 3: Faults excluded based on the proposed improved fault exclusion method. If faults are detected by Chi-square test, then calculate $w(i)$, $c(i)$ and $d(i)$ according to Equations (16), (18) and (19) respectively, and sort the $w(i)(i = 1, 2, \ldots, n)$ and $c(i)(i = 1, 2, \ldots, n)$ in descending order to get the vectors $\boldsymbol{w}$ and $\boldsymbol{c}$, and sort $d(i)$ $(i = 1, 2, \ldots, n)$ in an ascending order to get the vector $\boldsymbol{d}$.

Steps 4: Faults excluded according to consensus voting model Equation (20). If the identification results of the three methods meet the model Equation (20), exclude the identified fault without checking it backwards, and then go to *Step 1* and continue to detect and exclude the other faults.

https://doi.org/10.1017/S0373463318001133 Published online by Cambridge University Press

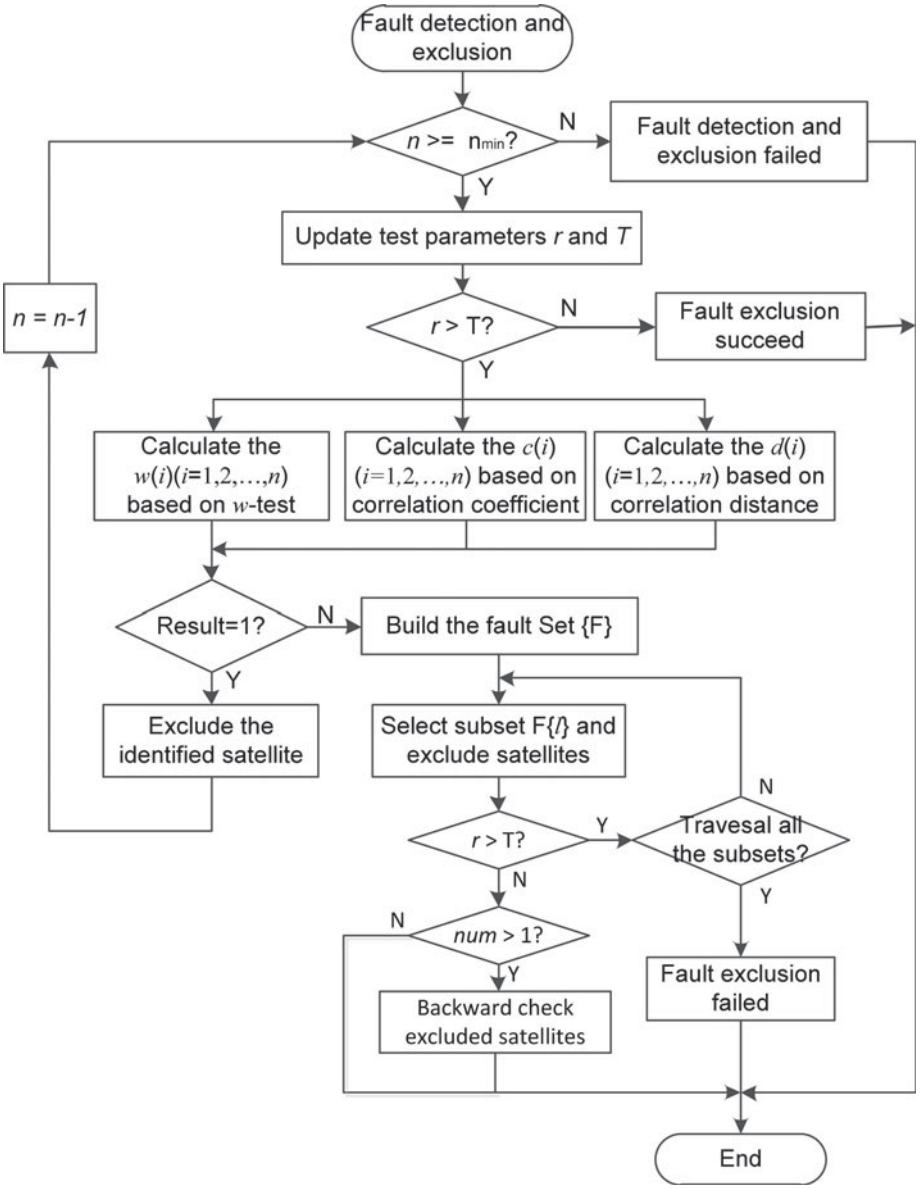

Figure 3. Flow chart of the improved fault detection and exclusion algorithm.

Step 5: Faults excluded based on fault set {F} . In Step 4, if the identification results of the three methods do not meet the model Equation (20), build a fault set {F} which contains all possible combinations of faults, and then exclude the possible faults according to the subset F{l} obtained from the {F} until $r \leq$T or all the subsets are traversed. If $r \leq$T and the number of excluded faults $num > 1$, backward check the excluded satellites or observations. If all the subsets are traversed, and there are still faults, the fault exclusion failed.

https://doi.org/10.1017/S0373463318001133 Published online by Cambridge University Press

6. TEST AND EXPERIMENT ANALYSIS. In this section, we first validate the effectiveness of the proposed consensus voting model by statistical analysis, and then further evaluate the performance of the improved fault detection and exclusion method by comparing the conventional methods based on GPS and BDS data with different simulated numbers of faulty satellites.

6.1. *Effectiveness of consensus voting model.* In order to verify the effectiveness of the consensus voting model described by Equation (20), we selected six IGS reference stations with GPS and BDS data. They are the stations JFNG (Wuhan, China), CUT0 (Curtin, Australia), NNOR (Perth, Australia), GMSD (Tanegashima, Japan), WARK (Warkworth, New Zealand) and REUN (Reunion, Indian Ocean). The stations' distribution is shown in Figure 4. The data span used covers seven days from 1–7 January 2017, and the sampling rate was every 30 s. The data sets cover a range of six to 23 visible satellites and Geometric Dilution of Precision (GDOP) from 1·0 to 20.

We simulated a different number of outliers for single GPS, BDS and combined GPS/BDS, and used the *w*-test, the correlation coefficient and the correlation distance methods to identify the outliers. The value of the bias for outliers was set to $1{\cdot}5\nabla b_i$, where ∇b_i is the minimum detectable bias of the i-th measurement, which is calculated by Equation (15). Assuming $k1$, $k2$ and $k3$ are the identification results of the three methods at the first-time exclusion, the significance level β is set as 0·01 for the correlation coefficient significance test. We acquired the probabilities that $k1$, $k2$ and $k3$ meet the following three situations in the case of different number of outliers respectively and calculated the corresponding correct probability of identification.

Situation 1: the identification results of the three methods meet $k1 = k2$ and $k2 = k3$.

Situation 2: the identification results meet $k1 = k2$ or $k2 = k3$, and the correlation coefficient is greater than the detection threshold with significance level $\beta = 0{\cdot}01$.

Situation 3: the identification results meet $k1 = k2$ or $k2 = k3$, but correlation coefficient is less than the detection threshold with significance level $\beta = 0{\cdot}01$.

Figure 5 shows that the probability that the identification results of the three methods meet situation 1 decreases with the increases of the number of outliers. Instead, the probabilities that the identification results of the three methods meet situations 2 and 3 increases with the number of outliers. The statistical results show that the consistency of the identification results of the three methods decreases with the increase of the number of outliers. Moreover, the total probability that the identification results of the three methods meet situations 1 and 2 for combined GPS/BDS is greater than for single GPS and BDS in the case of the same number of outliers, which indicates that the consistency of the identification results of the three methods for combined GPS/BDS is better than for single GPS and BDS. The correct identification probabilities in situations 1, 2 and 3 are shown in Figures 7, 8 and 9. It is shown by statistical results that the correct identification probability that the identification results of the three methods meet the situation 1 or 2 are all greater than 99%, while the correct identification probability in situation 3 is in a range from 20% to 95%. So, the fault identification result is reliable when the identification results of the three methods meet either situation 1 or situation 2 that form the consensus voting model. Consequently, the consensus voting model is useful for determining the outliers.

6.2. *Performance test based on real data with single fault.* The satellite identifiers of GPS and BDS are from C01 to C32 and C33 to C67 respectively. A real BDS satellite C34 failure occurred on 2 November 2016. Therefore, the data of the day from station JFNG

https://doi.org/10.1017/S0373463318001133 Published online by Cambridge University Press

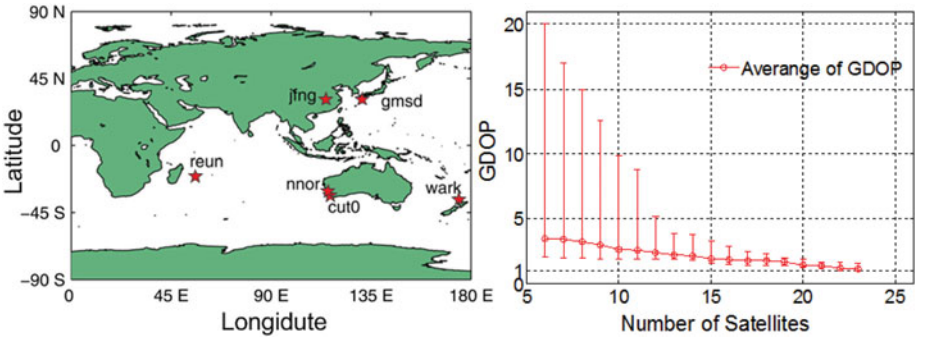

Figure 4. Stations distribution and data sets covering the number of visible satellites and the corresponding GDOP.

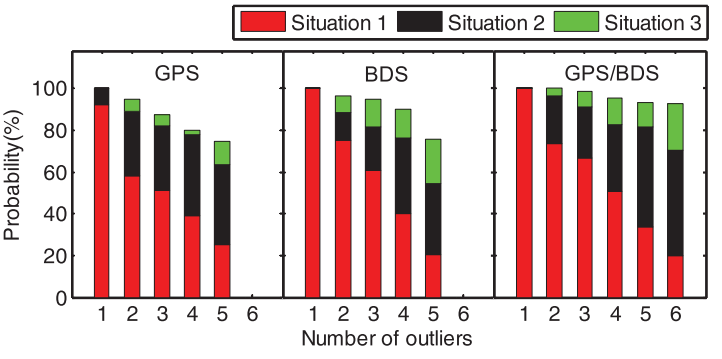

Figure 5. Probability that the identification results of the three methods meet Situations 1, 2 and 3 in the case of different numbers of outliers for GPS, BDS and GPS/BDS.

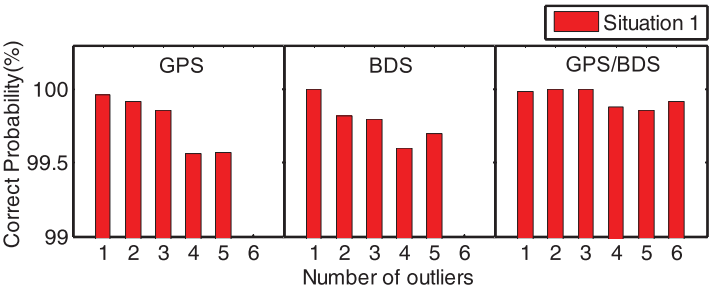

Figure 6. Correct identification probability based on GPS, BDS and GPS/BDS with different numbers of outliers in situation 1.

is used to verify the performance of the improved method in the case of a single fault. The number of the visible satellites and GDOP of GPS, BDS and GPS/BDS are shown in Figure 9.

The Chi-square test was used to detect the fault and the significance level a was set to 0·001, namely P_{FA} = 0·001. As can be seen from Figure 10, the positioning errors of BDS and GPS/BDS from epochs 781 to 821 have an obvious increase, but the positioning errors

https://doi.org/10.1017/S0373463318001133 Published online by Cambridge University Press

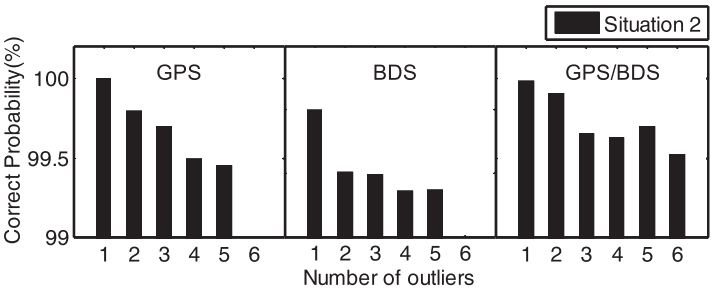

Figure 7. Correct identification probability based on GPS, BDS and GPS/BDS with different numbers of outliers in situation 2.

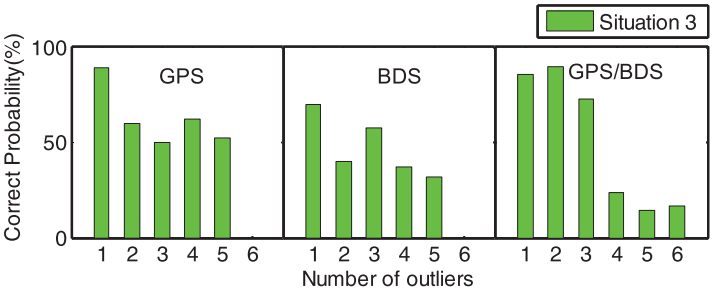

Figure 8. Correct identification probability based on GPS, BDS and GPS/BDS with different numbers of outliers in situation 3.

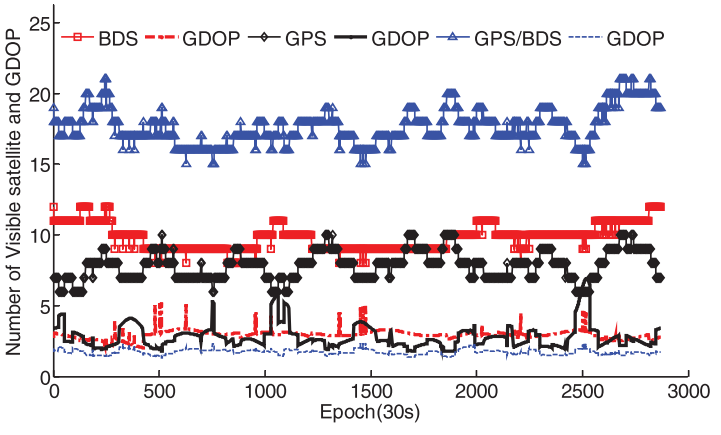

Figure 9. Number of visible satellites and GDOP at each epoch (cut angle 15°).

of GPS do not show a significant change. In addition, the results of the Chi-square test in Figure 11 show that the WSSR of BDS and GPS/BDS are all larger than the corresponding threshold from epochs 781 to 821. Accordingly, we can determine that there should be a fault in BDS from epoch 781 to 821. Moreover, we can also find from Figure 10 that the positioning accuracy of the combined GPS/BDS is better than that of a single system GPS or BDS due to having more observations in the case of no outliers in observations.

https://doi.org/10.1017/S0373463318001133 Published online by Cambridge University Press

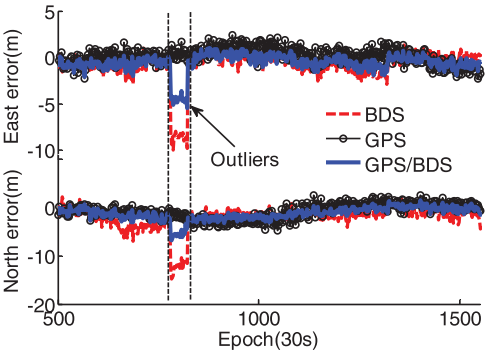

Figure 10. Positioning error sequence in E and N directions for GPS, BDS and GPS/BDS.

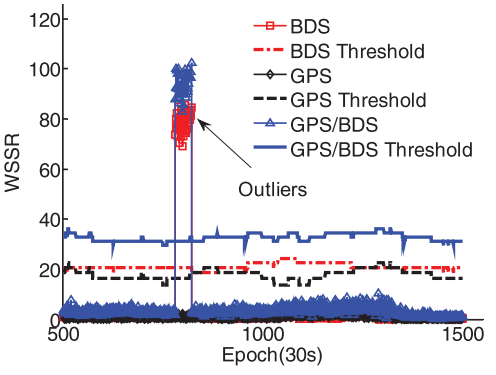

Figure 11. Results of Chi-square test for GPS, BDS and GPS/BDS.

Table 2. Identification results and performance of the four methods.

Methods	Faulty identifier	Fault epochs	Correct probability(%)	Average times
FDE-*c*	C34	781–821	100%	1·05
FDE-*d*	C34	781–821	100%	1·25
FDE-*w*	C34	781–821	100%	1·10
FDE-*u*	C34	781–821	100%	1·05

However, the positioning accuracy will be reduced when there is a fault in GPS or BDS. So, FDE is important in improving the positioning accuracy. We used the conventional methods and our improved method to detect and exclude the faults, respectively. The identification results, correction identification probability and computation complexity of each methods are listed in Table 2. In order to use statistics easily, the computational complexity is simply represented by the average times of Chi-square test performed to achieve fault exclusion. Figures 12 and 13 show the positioning errors and the results of the Chi-square test after fault exclusion by using the improved method. The results show that the four methods can all identify the faulty satellite correctly. However, FDE-*c* and FDE-*u* methods have higher efficiency.

https://doi.org/10.1017/S0373463318001133 Published online by Cambridge University Press

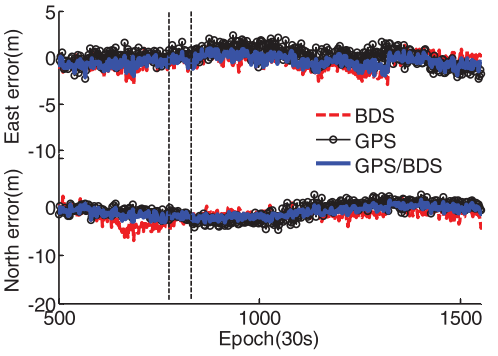

Figure 12. Positioning error sequence in E and N directions after fault exclusion by FDE-u.

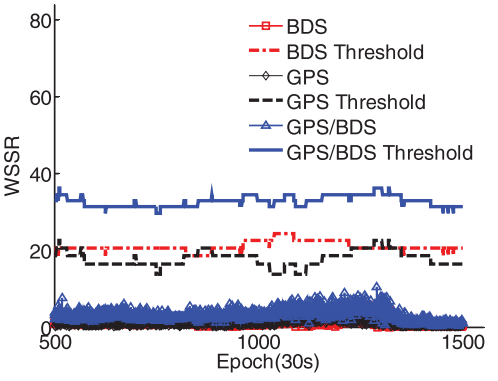

Figure 13. Results of Chi-square test after fault exclusion by FDE-u.

6.3. *Performance test based on simulation data with multiple faults.* To better understand the performance of the improved method under the condition of single GNSS constellation and multiple GNSS constellations, we used GPS, BDS and GPS/BDS data to test and compare the performance of the conventional methods and the improved method in the case of a different number of faults. In each experiment, we used the Monte Carlo method to simulate the faults and count the false exclusion probability, correct exclusion probability and the computation complexity of each method. False exclusion occurred when the excluded satellites by fault exclusion methods did not all have faults. A correct exclusion is defined as when all the faulty satellites were excluded correctly. The Chi-square test was also used to detect faults and the value of bias for simulated faults was set to $1{\cdot}5\nabla b_i$. Table 3 lists the identification results of the four methods at various epochs. The results show that in the case of multiple faults, the FDE-*c*, FDE-*d* and FDE-*w* methods sometimes appeared to yield false identification or failed identification and had different identification results. The correlation analysis methods had a better performance than the *w*-test method in the condition of multiple faults. Table 4 shows a performance comparison of the four methods with a different number of faults. The symbol "×" indicates that there was invalid data.

As can be seen from Table 4 and Figure 14, for the single GPS system, the correct identification probability of the improved method was greater than 99% in the case of two

https://doi.org/10.1017/S0373463318001133 Published online by Cambridge University Press

Table 3. Identification results of the four methods at various epochs.

Epoch	System	No. of Satellite	Faulty identifier	Methods			
				FDE-*c*	FDE-*d*	FDE-*w*	FDE-*u*
367	GPS	7	2, 17	2, 17	5, 17	2, 19	2, 17
181	BDS	11	33, 34	33, 34	33, 34	35, 36, 37	33, 34
177	GPS	8	2, 6, 17	2, 6, 17	failed	2, 19, 28	2, 6, 17
242	BDS	12	33, 35, 38	33, 37, 42, 43, 45, 46	35, 37, 42, 43, 46	35, 33, 40, 41, 42, 43	35, 33, 38
857	GPS	9	2, 5, 13, 15	failed	failed	20, 21, 24, 29	2, 5, 13, 15
201	BDS	11	33, 34, 35, 36	33, 34, 36, 37, 38, 43	33, 34, 35, 36	35, 36, 38, 41, 42, 43	33, 34, 35, 36

Table 4. Performance comparison of the four methods.

No. of Faults	Method	False Probability (%)			Correct Probability (%)			Average times		
		GPS	BDS	GPS/BDS	GPS	BDS	GPS/BDS	GPS	BDS	GPS/BDS
2	FDE-*c*	7·2	0·0	0·0	92·1	100	100	4·06	4·00	4·00
	FDE-*d*	13·3	0·0	0·0	73·3	100	100	4·01	4·00	4·00
	FDE-*w*	25·7	3·2	0·0	67·2	94·3	100	4·26	4·06	4·00
	FDE-*u*	0·1	0·0	0·0	99·8	100	100	3·03	2·30	2·58
3	FDE-*c*	15·2	25·5	0·0	79·1	58·6	100	6·01	6·30	6·11
	FDE-*d*	13·8	6·3	0·0	72·2	92·5	100	6·00	6·05	5·98
	FDE-*w*	41·6	40·9	0·4	21·2	37·7	98·1	6·50	7·39	6·25
	FDE-*u*	1·20	0·3	0·0	96·3	99·1	100	5·56	5·91	3·89
4	FDE-*c*	5·3	20·2	0·0	36·2	79·2	100	8·2	8·15	8·13
	FDE-*d*	4·1	36·6	0·2	52·1	26·5	99·7	8·15	7·91	8·11
	FDE-*w*	3·2	46·3	2·8	17·7	30·1	97·0	8·25	8·48	8·37
	FDE-*u*	3·8	3·3	0·0	91·3	95·4	100	8·33	8·05	5·51
5	FDE-*c*	×	×	0·16	×	×	99·8	×	×	10·12
	FDE-*d*	×	×	1·12	×	×	98·6	×	×	9·98
	FDE-*w*	×	×	18·6	×	×	77·7	×	×	11·15
	FDE-*u*	×	×	0·0	×	×	100	×	×	8·08
6	FDE-*c*	×	×	0·37	×	×	99·5	×	×	12·13
	FDE-*d*	×	×	4·52	×	×	94·0	×	×	12·41
	FDE-*w*	×	×	55·7	×	×	40·2	×	×	13·09
	FDE-*u*	×	×	0·0	×	×	100	×	×	11·45

faults, which increased by 8% compared with the FDE-*c* method. The correct identification probability was greater than 90% with three or four faults. Compared with the conventional methods it increased by 20% to 50%. According to Table 4 and Figure 15, we can find that, for the single BDS system, the correct identification probability of the improved method was nearly 100% in the case of two faults, and the correct identification probability was greater than 95% within three or four faults, increasing 5% to 15% compared with the conventional methods. In addition, Table 4 and Figure 16 show that, for the combined GPS/BDS system, the correct identification probability of the improved method was almost 100% in the case of less than six faults. Comparing with the conventional methods, the computational efficiency of the improved method is reduced by almost half in the case of

https://doi.org/10.1017/S0373463318001133 Published online by Cambridge University Press

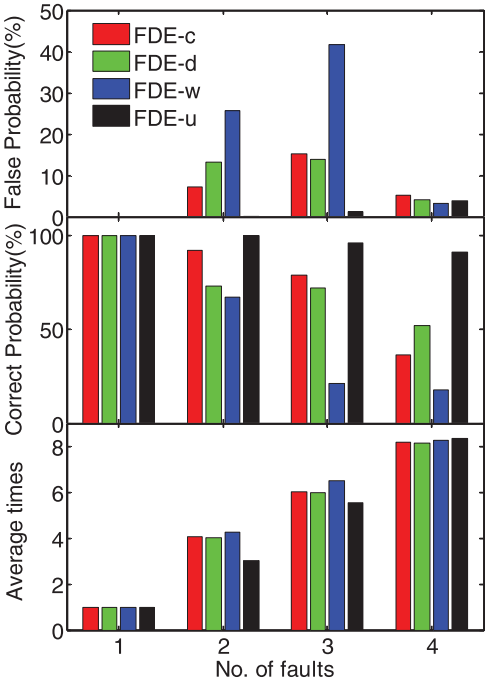

Figure 14. Performance of the four methods based on GPS data with different numbers of faults.

two faults, but it is not significantly reduced in the case of more than three faults under the condition of the single GNSS system.

The statistical results show that the correct identification probability decreases and that the computational complexity of the four methods increased with the number of faults. However, under the same condition, the improved method has higher correct identification probability, lower false identification probability and higher efficiency compared with the other three methods. The results also show that the correct identification probability of the improved method based on the single GPS system is lower than that based on the single BDS system. This is because the number of visible GPS satellites is lower than in the case of BDS at a given epoch, resulting in poor redundant observation in some epochs, which can be seen from Figure 9. In addition, the performance of the improved method based on a multiple GNSS system constellation is better than for a single GNSS system.

7. CONCLUSIONS. The conventional RAIM algorithms are theoretically based on the assumption that only one fault happens. They generally have a lower correct identification probability in the case of multiple faults. Although there has been a previous reliability theory for multiple faults, it is effective only in regard to two faults. In the case of multiple faults, the conventional RAIM algorithms often use the forward-backward method based on a *w*-test or correlation analysis to exclude multiple faults. However, they have a lower efficiency and often give erroneous identifications. This paper presents an improved method for excluding single and multiple faults based on consensus voting using the *w*-test,

https://doi.org/10.1017/S0373463318001133 Published online by Cambridge University Press

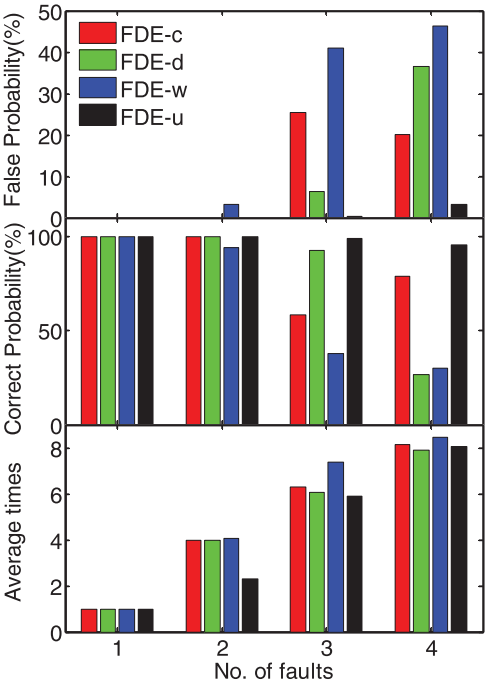

Figure 15. Performance of four methods based on BDS data with different numbers of faults.

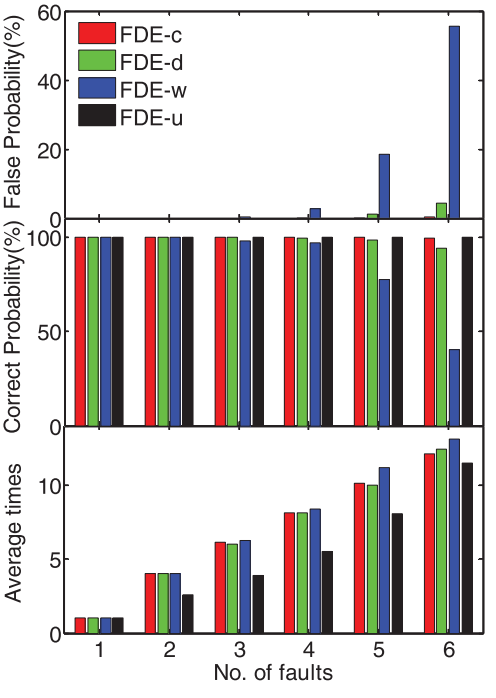

Figure 16. Performance of four methods based on GPS/BDS with different numbers of faults.

https://doi.org/10.1017/S0373463318001133 Published online by Cambridge University Press

the correlation coefficient, and the correlation distance methods, which combines the identification results of the three methods to achieve fault exclusion. If the identification results of the three methods meet the consistency conditions, the probability of false identification will be very low. Therefore, we can determine that the identification result is a fault and exclude it without a need to conduct a backward check. If the identification results of the three methods fail to meet the condition of the consistency check, one needs to traverse the collection of faults to exclude the faults. The method is invalid if all the fault subsets are traversed but there are still faults. The experiment results have demonstrated that the improved method has the same performance as the conventional methods in the case of single fault and has higher efficiency and identification accuracy in the case of multiple faults than conventional methods.

ACKNOWLEDGMENTS

This project is supported by the National Natural Science Foundation of China (Grants No. 41274038, 41574024), the National Science and Technology Major Project of the National Key R&D Program of China (Grant No.2016YFB0502102), the Beijing Natural Science Foundation (Grant No. 4162035), the Aeronautical Science Foundation of China (Grant No. 2016ZC51024) and the Academic Excellence Foundation of BUAA for PhD students.

REFERENCES

Baarda, W. (1968). A testing procedure for use in geodetic networks. Netherlands Geodetic Commission, Publication on Geodesy, New Series 2, No. 5, Delft, Netherlands.

Bei, J.Z., Gu, S.Z. and Fang, S.S. (2010). A new RAIM method based on vector correlation distance, *Scientia Sinica (Physica, Mechanica & Astronomica)*, **40**, 638–643.

Brown, R.G. (1992). A Baseline GPS RAIM Scheme and a Note on the Equivalence of Three RAIM Methods. *Navigation*, **39**, 301–316. doi:10.1002/j.2161-4296.1992.tb02278.x

Brown, R.G. and McBurney, P.W. (1988). Self-contained GPS integrity check using maximum solution separation. *Navigation*, **35**, 41–53. doi:10.1002/j.2161-4296.1988.tb00939.x

Cao, K., Hu, Y., Xu, J. and Li, B. (2013) Research on improved RAIM algorithm based on parity vector method. *International Conference on Information Technology and Applications*, Taiyuan, China, 221–224.

Chen, J.P., Wang, J., Zhang, Y.Z., Yang, S.N., Chen, Q. and Gong, X.Q. (2016). Modeling and Assessment of GPS/BDS Combined Precise Point Positioning. *Sensors*, **16**, 1151–1163.

DeGroot, M.H and Schervish, M.J. (2011). *Probability and Statistics*. Pearson Education, Beijing.

Feng, S.J., Ochieng, W.Y., Walsh, D. and Ioannides, R. (2006) A measurement domain receiver autonomous integrity monitoring algorithm, *GPS Solutions*, **10**, 85–96. doi:10.1007/s10 291-005-0010-8

Filliben, J.J. (1975). The probability plot correlation coefficient test for normality. *Technometrics*, **17**, 111–117. doi:10.1080/00401706.1975.10489279

Hewiston, S. and Wang, J.L. (2006). GNSS receiver autonomous integrity monitoring (RAIM) performance analysis. *GPS Solutions*, **10**, 155–170. doi:10.1007/s10291-005-0016-2

Hewitson, S., Lee, H.K. and Wang, J.L. (2004). Localizability analysis for GPS/Galileo receiver autonomous integrity monitoring. *The Journal of Navigation*, **57**, 245–259. doi:10.1017/S0373463304002693

Hu, Y.F., Lu, J.J., Cao, K.J. and Li, B. (2014). RAIM algorithm based on correlation distance with several epoch. *Journal of Detection & Control*, **36**, 42–45.

Innac, A., Bhuiyan, M.Z.H., Söderholm, S., Kuusniemi, H. and Gaglione, S. (2016). Reliability testing for multiple GNSS measurement outlier detection. *European Navigation Conference*, Helsinki, Finland, 530–540. doi:10.1109/EURONAV.2016.7530540

Joerger, M. and Pervan, B. (2014). Solution separation and Chi-Squared ARAIM for fault detection and exclusion. *Proc. IEEE/ION PLANS 2014*, Institute of Navigation, Monterey, CA, USA, May 5–8, 294–307.

Kaplan, E.D. and Hegarty, C.J. (2006). *Understanding GPS: principles and applications*. Artech House, London.

Knight, N.L., Wang, J.L. and Rizos, C. (2009). GNSS integrity monitoring for two satellite faults. *IGNSS Symposium 2009*, Surfers Paradise, Australia, 221–224.

Knight, N.L., Wang, J.L. and Rizos, C. (2010). Generalised measures of reliability for multiple outliers. *Journal of Geodesy*, **84**, 625–635. doi:10.1007/s00190-010-0392-4

Kuusniemi, H., Wieser, A., Lachapelle, G. and Takala, J. (2007). User-Level Reliability Monitoring in Urban Personal Satellite-Navigation. *IEEE Transactions on Aerospace & Electronic Systems*, **43**, 1305–1318.

Lee, Y.C. (1986). Analysis of range and position comparison methods as a means to provide GPS integrity in the user receiver. *Proceedings of ION GPS 1986*, Institute of Navigation, Seattle, Washington, June 24–26, 1–4.

McAllister, D.F., Sun, C.E. and Vouk, M.A. (1990). Reliability of voting in fault-tolerant software systems for small output-spaces. *IEEE Transactions on Reliability*, **39**, 524–534. doi:10.1109/24.61308

McBurney, P.W. and Brown, R.G. (1989). Self-contained GPS integrity monitoring using a censored Kalman filter. *Proceedings of ION GPS 1988*, Institute of Navigation, Colorado Spring, CO, September 19–23, 441–450.

Ni, J., Zhu, Y. and Guo, W. (2007). An improved RAIM scheme for processing multiple outliers in GNSS. *International Conference on Advanced Information Networking and Applications Workshops*, Niagara Falls, Ont., Canada, 840–845.

Pan, Z., Chai, H. and Kong, Y. (2017). Integrating multi-GNSS to improve the performance of precise point positioning. *Advances in Space Research*, **60**, 2596–2606. doi:10.1016/j.asr.2017.01.014

Parkinson, B. and Penina, A. (1988). Autonomous GPS integrity monitoring using the pseudorange residual. *Navigation*, **35**, 255–274. doi:10.1002/j.2161-4296.1988.tb00955.x

Ren, D. and Ching-Fang, L. (1995). A new failure detection approach and its application to GPS autonomous integrity monitoring. *IEEE Transactions on Aerospace and Electronic Systems*, **31**, 499–506. doi:10.1109/7.366336

Salos, D., Martineau, A., Macabiau, C., Bonhoure, B. and Kubrak, D. (2014). Receiver Autonomous Integrity Monitoring of GNSS signals for electronic toll collection. *IEEE Transactions on Intelligent Transportation Systems*, **15**, 94–103. doi:10.1109/tits.2013.2273829

Sturza, M.A. (1988). Navigation system integrity monitoring using redundant measurements. *Navigation*, **35**, 483–501. doi:10.1002/j.2161-4296.1988.tb00975.x

Takasu, T. and Yasuda, A. (2013). RTKLIB ver. 2.4.2 Manual. http://www.rtklib.com/rtklib.htm.

Tang, Y.M., Wang, J. and Peng, X.G. (2011). Research on integrated navigation RAIM model based on correlation analysis. *Journal of Geodesy and Geodynamics*, **31**, 139–143.

Wang, H. (2015). An Improved RAIM algorithm on simultaneous two-faulty satellites. *2015 8th International Symposium on Computational Intelligence and Design (ISCID)*, Hangzhou, China, 643–648.

Yang, L., Li, Y., Wu, Y. and Rizos C. (2014). An enhanced MEMS-INS/GNSS integrated system with fault detection and exclusion capability for land vehicle navigation in urban areas. *GPS Solutions*, **18**, 593–603. doi:10.1007/s10291-013-0357-1

Yang, Y. and Xu, J. (2016). GNSS receiver autonomous integrity monitoring (RAIM) algorithm based on robust estimation. *Geodesy and Geodynamics*, **7**, 117–12.

Yang, L., Wang, J., Knight, N. L. and Shen, Y.Z. (2013). Outlier separability analysis with a multiple alternative hypotheses test. *Journal of Geodesy*, **87**, 591–604. doi:10.1007/s00190-013-0629-0

Yoo, J., Ahn, J., Lee, Y.J. and Sung, S. (2012). Performance Comparison of GPS Fault Detection and isolation via pseudorange prediction model based test statistics. *Journal of Electrical Engineering & Technology*, **7**, 797–806. doi:10.5370/JEET.2012.7.5.797

Zhao, L., Gao, N., Huang, B. and Wang, Q. (2015). A Novel Terrain-Aided Navigation Algorithm Combined With the TERCOM Algorithm and Particle Filter. *IEEE Sensors Journal*, **15**, 1124–1131. doi:10.1109/JSEN.2014.2360916